

# Sculpturing of a non-spreading wave packet in imaginary potentials

R. Stützle,\* M.C. Göbel, Th. Hörner, E. Kierig, I. Mourachko, and M.K. Oberthaler  
*Kirchhoff-Institut für Physik, Universität Heidelberg,  
Im Neuenheimer Feld 227, D-69120 Heidelberg, Germany†*

M.A. Efremov,<sup>1</sup> M.V. Fedorov,<sup>1</sup> V.P. Yakovlev,<sup>2</sup> K.A.H. van Leeuwen,<sup>3</sup> and W.P. Schleich<sup>4</sup>  
<sup>1</sup>*General Physics Institute, Russian Academy of Sciences, 38 Vavilov st, Moscow, 119991 Russia*  
<sup>2</sup>*Moscow Engineering Physics Institute (State University), 31 Kashirskoe shosse, Moscow, 115409 Russia*  
<sup>3</sup>*Eindhoven University of Technology, P.O. Box 513, 5600 MB Eindhoven, The Netherlands and*  
<sup>4</sup>*Abteilung für Quantenphysik, Universität Ulm, D-89069 Ulm, Germany*

(Dated: December 2, 2024)

We propose and experimentally demonstrate a method to prepare a non-spreading atomic wave packet. Our technique relies on a spatially modulated absorption constantly chiselling away from an initially broad de-Broglie wave. Heisenberg's uncertainty principle puts a limit to this contraction and determines the final complex Gaussian form of the packet. Experimentally we confirm the predicted formation process of the wave packet by observing the evolution of the momentum distribution. Moreover by employing interferometric techniques we measure the predicted quadratic phase across the wave packet.

PACS numbers: 03.75.Be, 42.50.Vk, 03.75.Dg

To sculpture means for Michelangelo releasing the desired form from a block of marble by cutting away unwanted materials [1]. This summary of Michelangelo's creative work highlights not only the mechanical aspect of sculpturing but also its artistic component: to recognize what should be left. In this spirit of Michelangelo we propose and experimentally demonstrate a method to prepare an atomic wave packet. Our de-Broglie sculpturing technique relies on three ingredients: (i) an absorption process cuts away the unwanted parts of a broad wave creating a packet that is continuously contracting in position space, (ii) this process leads due to Heisenberg's uncertainty relation to a broadening in momentum space and consequently to a faster spreading in real space, and (iii) the absorptive sculpturing and the quantum diffusion are balanced leading to a non-spreading wave packet. Hence, the absorption plays the role of the mechanical work while Heisenberg's uncertainty principle defines the final form released from the original de-Broglie wave.

Non-spreading wave packets have attracted interest since the early days of quantum mechanics. Three examples may serve as an illustration: (i) In 1926 Schrödinger [2] found that the displaced Gaussian ground state of a harmonic oscillator, that is a coherent state, experiences conformal evolution in this potential. (ii) The invariance of an Airy-function-shaped freely moving wave packet [3] results from correlations between position and momentum stored in the initial wave function. (iii) The Trojan wave packet [4] of an atomic electron is held together by a balance of the Coriolis force and a time dependent external electric field.

The Michelangelo wave packet combines the key features of all three above mentioned packets. As the Schrödinger coherent state it is caught in an effective harmonic oscillator potential [5]. However, in our case

it is the pure imaginary potential. Correlations between position and momentum dictated by Heisenberg's uncertainty relation are vital for the Airy wave. They are also of central importance for the Michelangelo packet. Moreover, the latter, like the Trojan packet, is exposed to a time dependent electric field, but of optical frequency which leads to an effective absorptive potential.

A model system for engineering non-dispersive electronic wave packets are Rydberg atoms [7]. A non-spreading, slowly decaying wave packet supported by an external field arises [8] in the case of interference stabilization, when a Rydberg atom is photoionized by a sufficiently strong light field. Another realization [9] relies on phase locking the motion of the outer electron to the inner electron in a two-electron planetary atom. Spreading of a bound electronic wave packet can also be suppressed [10] via phase locking in a weak near-resonant microwave field.

In some sense our method of Michelangelo sculpturing is related to the technique suggested in [11] to obtain a non-spreading wave packet in a two-electron atom using atomic mode locking by loss modulation. In the latter the Rabi oscillations of the core electron induced by an external field modify the autoionization of the outer electron when it approaches the core. In this way the tails of the orbiting wave packet get ionized and only its center survives. This cutting procedure repeats itself with the Kepler period. Hence, Michelangelo sculpturing appears as the continuous version of this technique extended to the center-of-mass motion of neutral atoms rather than bound electrons.

Atom optics [12, 13] realizes complex potentials for matter waves [14, 15, 16, 17] by the interaction of near resonant light with an open two-level system shown in Fig. 1a. For a standing light wave tuned *exactly* on reso-

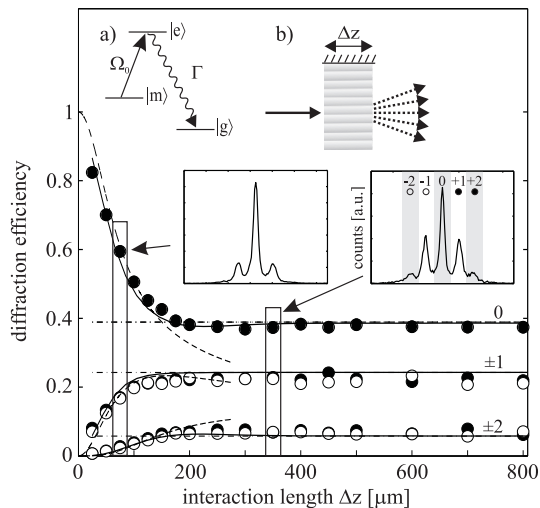


FIG. 1: Formation of a non-spreading Michelangelo wave packets for the center-of-mass motion of an open two-level atom (a). The resonant interaction with a standing light wave (b) leads to an array of harmonic imaginary potentials. The normalized diffraction efficiencies derived from the momentum distributions (inset) approach a steady state as a function of the interaction length  $\Delta z$  demonstrating the successful realization of stationary wave packets. The solid curves result from a numerical integration of the Schrödinger equation [6] with the Rabi frequency  $\Omega_0 = 0.4\Gamma$ . The dashed lines correspond to the Raman-Nath approximation, revealing that the interplay between absorption and quantum diffusion is essential for obtaining a steady state.

nance an array of purely imaginary harmonic potentials arises. When the Rabi frequency  $\Omega_0$  is of the order of the excited state linewidth  $\Gamma$  the local saturation parameter  $|\Omega_0 \sin(kx)/\Gamma|$  and thus the upper level population is of the order of unity except in a small vicinity of the field nodes. Consequently our system decays approximately with the rate  $\Gamma$ . Therefore, in the time domain  $t \gg 1/\Gamma$  the atomic wave function vanishes almost everywhere, except in small vicinity  $\delta x$  of the field nodes. Here the saturation is small and our open system decays with the rate  $(\Omega_0 k \delta x)^2/\Gamma \ll \Gamma$ . We estimate the time dependent size  $\delta x$  from the relation  $(\Omega_0 k \delta x)^2 t/\Gamma \sim 1$  and find  $\delta x(t) \sim (\Gamma/t)^{1/2}/(k\Omega_0)$ .

The decrease of  $\delta x(t)$  is accompanied by an increase of the width  $\delta p(t) \sim 1/\delta x(t)$  in momentum space [18] leading to spatial spreading of the wave packet. Due to competition of the two processes - absorptive contraction and quantum diffusion - the width  $\delta x(t)$  reaches its minimal stationary value  $\delta x_0$ . In this asymptotic regime the rate  $\delta x(t)/t$  of absorptive contraction is obviously balanced by the rate  $\delta p(t)/M$  of quantum diffusion which yields the characteristic time

$$t_0 \equiv 1/\omega_0 \sim \frac{1}{\Omega_0} \sqrt{\frac{\Gamma}{\omega_r}} \quad (1)$$

and the stationary width

$$\delta x_0 \sim \frac{1}{\sqrt{M\omega_0}} \quad (2)$$

with the recoil frequency  $\omega_r \equiv k^2/(2M) \ll \Gamma$ .

The experiments are performed with a slow atomic beam of metastable argon ( $v = 50$  m/s) produced with a standard Zeeman-Slower. The brilliance of the beam is significantly enhanced with a 2D-MOT setup [19]. The final collimation necessary for coherent illumination is obtained by two slits ( $25 \mu\text{m}$  and  $10 \mu\text{m}$ ) within a distance of 25 cm. Applying a Stern-Gerlach magnetic field we select the atoms in the internal state  $1s_5$  ( $J = 2, m_j = 0$ ). The imaginary potential is realized with a circularly polarized standing light wave by retro reflecting a laser beam resonant with the  $1s_5-2p_8$  transition (801 nm). This setup realizes to a very good approximation an open two-level system since only 16% of the excited atoms fall back to the initial state (in contrast to 32% without magnetic state selection). In order to control the interaction length  $\Delta z$  the laser beam passes an adjustable slit. By imaging the slit onto the retro-reflecting mirror we avoid the spoiling effect of light diffraction. The detection of the metastable argon atoms is achieved by a micro-channel-plate-detector allowing for spatially resolved single atom detection utilizing the internal energy (12 eV). Since the transverse coherence length of the incoming atomic beam is much larger than the optical wave length the outgoing wave function is a coherent array of single Michelangelo wave packets, resulting in constructive interference in certain directions. The spatial resolution  $\sim 50 \mu\text{m}$  of our atomic detector and the free flight distance  $\sim 0.5$  m guarantee to clearly resolve the resulting atomic diffraction pattern in the far field.

The diffraction efficiency is deduced by summing up the detected number of atoms in angular windows as indicated in the right inset of Fig. 1. After initial dynamics the wave packets i.e. the diffraction efficiencies do not change giving evidence to the formation of Michelangelo wave packets [20]. Our numerical simulations (solid line) of the open two-level Schrödinger equation take into account the longitudinal as well as the transverse velocity distributions  $\Delta v_l = 10$  m/s and  $\Delta v_t = 7$  mm/s of the experiment. For  $\Omega_0 = 0.4\Gamma$  we have a very good agreement with our experimental findings. Since this agreement depends critically on the Rabi frequency we can determine its absolute value. It is consistent within a factor of two both with a rough estimate using the power measurement of the incoming light beam and with the overall absorption of the atomic beam.

In order to stress that the interplay between absorptive narrowing and the quantum diffusion is crucial for the formation of the Michelangelo packet, we have included the result of the Raman-Nath approximation (dashed lines). Since this approach is only valid as long as quantum diffusion is negligible, it fails to predict the resulting

dynamics after the characteristic time  $t_0$ .

According to Eq. (1) Michelangelo wave packets emerge after a characteristic time  $t_0 \sim 1/\Omega_0$ . Our experimental results shown in Fig. 2 confirm the expected scaling with  $\Omega_{min} = 0.23\Gamma$ .

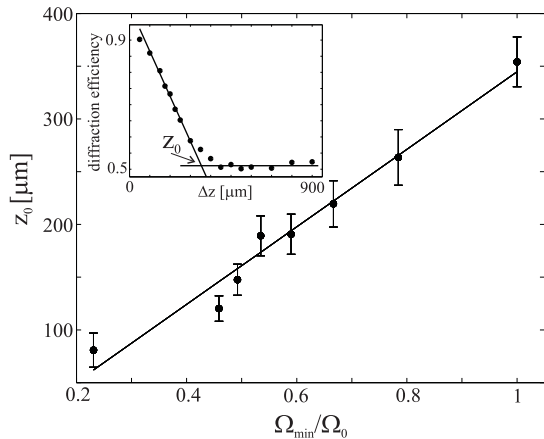


FIG. 2: Experimental verification of the scaling law  $t_0 \sim 1/\Omega_0$  connecting the characteristic time  $t_0 \equiv z_0/v$  when Michelangelo wave packets form and the Rabi frequency  $\Omega_0$ . The line is a guide to the eye. We measure the zeroth order diffraction efficiency as a function of  $\Delta z$  (inset) for different Rabi frequencies. The crossing point between the linear extrapolation of the short and long time limits yields  $z_0$ .

We now show that a Michelangelo wave packet is a complex Gaussian wave packet with a quadratic phase. For this purpose we recall [6] that the solution of the Schrödinger equation

$$i\frac{\partial}{\partial t}\varphi(x,t) = \left(-\frac{1}{2M}\frac{\partial^2}{\partial x^2} - i\frac{M\omega_0^2}{2}x^2\right)\varphi(x,t), \quad (3)$$

for the metastable state wave function  $\varphi(x,t)$  in the vicinity of  $x=0$  after the elimination of the excited state reads

$$\varphi(x,t) = \sqrt{\frac{k/\pi}{\cosh\beta t}} \exp\left(-\frac{1}{2}\alpha x^2 \tanh\beta t\right) \quad (4)$$

where  $\omega_0 \equiv \Omega_0 \sqrt{2\omega_r/\Gamma}$ ,  $\alpha \equiv M\omega_0 \exp(-i\pi/4)$  and  $\beta \equiv \omega_0 \exp(i\pi/4)$ . Hence, the probability density  $|\varphi(x,t)|^2$  is a Gaussian with the time dependent width  $\delta x(t) \equiv [\text{Re}\{\alpha \tanh(\beta t)\}]^{-1/2}$  which for  $\omega_0 > 1$  reaches its minimal stationary value

$$k\delta x_0 \equiv \left(2\frac{\omega_r^2}{\omega_0^2}\right)^{1/4} = \left(\frac{\omega_r\Gamma}{\Omega_0^2}\right)^{1/4}. \quad (5)$$

In this asymptotic regime Eq. (4) factorizes into a product of the time dependent function  $\cosh^{-1/2}(\beta t)$  showing that the Michelangelo probability density decays exponentially in time with the rate  $\Gamma_0 \equiv \omega_0/\sqrt{2} \ll \Gamma$ , and the position dependent complex Gaussian

$\exp(-\alpha x^2/2)$  which contains the quadratic phase  $\phi(x) \equiv M\omega_0 x^2/\sqrt{8}$ . A Fourier transformation of this wave packet with the stationary width, Eq. (5), yields the asymptotic behavior of the diffraction efficiencies shown in Fig. 1 by the dashed-dotted lines and is in perfect agreement with our experimental findings.

The predicted phase  $\phi(x)$  of the Michelangelo packet can be deduced from the phases of the observed diffraction orders where the phase of the  $n$ -th order with respect to the zeroth order is  $\phi(n) = -2(\omega_r\Gamma/\Omega_0^2)^{1/2}n^2 \equiv \phi_2 n^2$ . To measure the relative phases we realize a compact interferometer setup shown in Fig. 3a. A thin near resonant probing standing light wave (waist  $30\ \mu\text{m}$ ) is placed directly behind the array of harmonic imaginary potentials. The wave function amplitude in each output direction is given as a superposition of different diffraction orders of the Michelangelo packet. By changing the relative phase between the two standing light waves we can measure an interference pattern and thus deduce the phase evolution as a function of the interaction length  $\Delta z$ .

The interferometric setup employs a probing standing wave at  $801\ \text{nm}$  realized by beams impinging on the mirror under an angle of  $10^\circ$ . Thus moving the mirror allows us to scan the relative phase  $\phi_s$  between the probing and sculpturing light wave (beating period  $25\ \mu\text{m}$ ). The presence of a magnetic field in the interaction region enables us to realize a detuned ( $8\ \text{MHz}$ ) probing wave using the same laser for both standing light waves but different circular polarizations. By detuning the probing light wave the total flux through the interferometric setup is significantly increased in comparison to an exactly resonant probing field.

In order to deduce the absolute value of  $\phi_2$  we evaluate the interferometer output in the direction of the *third* diffraction order. For our experimental parameters this beam is always a *two-beam* interference of the first and second diffraction order of the array of Michelangelo packets. In contrast, the output in lower diffraction order directions is the result of *multiple-beam* interference and does not allow us easily to deduce the involved phases.

In order to find the phase difference  $\phi(2) - \phi(1)$  we have to eliminate the offset phase arising mainly from the fact that the probing light field is not infinitely thin. For this purpose we take the difference between the measured phase in the long-time limit of the sculpturing wave ( $\Delta z > 400\ \mu\text{m}$ ) and the phase for the experimentally achievable shortest interaction length ( $50\ \mu\text{m}$ ). For the Rabi frequency  $\Omega_0 = (0.23 \pm 0.02)\Gamma$  we find the experimental value  $|\phi(2) - \phi(1)| = 1.70 \pm 0.17$ , which is in agreement with the prediction of the numerical integration  $\phi(2) - \phi(1) = 3\phi_2$ , that is  $|\phi_2| = 0.57 \pm 0.1$ . Moreover the characteristic length  $z_0 \sim 400\ \mu\text{m}$  for leveling off the phases coincides with the one for leveling off the diffraction efficiencies. Furthermore by increasing the Rabi frequency to  $\Omega_0 = (0.4 \pm 0.05)\Gamma$  we experimentally deduce  $|\phi_2| = 0.32 \pm 0.08$  which is in very good agree-

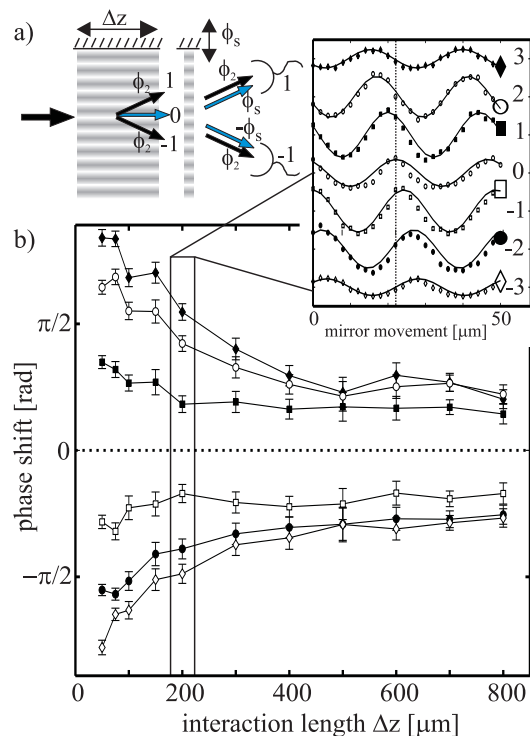


FIG. 3: Measurement of the phase of a Michelangelo wave packet using an interferometric setup (a) consisting of the sculpturing and probing standing waves. The inset in (b) shows typical interference patterns for different output directions obtained by scanning the relative position of the second (thin) standing light wave for a given interaction length  $\Delta z$ . For large values of  $\Delta z$  the phase shifts (b) of the different interferometer outputs relative to the zeroth order level off indicate stationary phases of the wave packet.

ment with the prediction of the numerical integration  $|\phi_2| = 0.27 \pm 0.04$ .

In conclusion we present a new class of non-spreading wave packets resulting from the interplay between absorptive narrowing and quantum diffusion. The developed theoretical description explains the experimental observation of both the phase and the amplitude of the wave packet very well. The experimental realization of imaginary potentials strongly relies on spontaneous decay processes. Nevertheless we show that coherence is maintained and can even be employed for deducing the phase of the Michelangelo packets. Since the wave packet arising in the long time limit is weakly dependent on the initial wave function this process is a robust tool for generating wave packets with well defined amplitude and phase for further experiments.

We acknowledge fruitful discussions with A. Buchleitner and thank M. Störzer for his commitment in the

early stage of the experiment which was funded by Optik-Zentrum Konstanz, Center for Junior Research Fellows in Konstanz, by Deutsche Forschungsgemeinschaft (Emmy Noether Program), and by the European Union, Contract No. HPRN-CT-2000-00125. WPS and VPY are enormously grateful to the hospitality of and the stimulating atmosphere at the Centro Internacional de Ciencias A.C. MVF, WPS and VPY also thank the Alexander von Humboldt-Stiftung for its generous support during the course of this project, especially for the Humboldt-Kolleg at Cuernavaca, Mexico. This work was partially supported by the Landesstiftung Baden-Württemberg and the Russian Foundation for Basic Research (grants no. 02-02-16400, 03-02-06145, 04-02-16734).

\* Electronic address: stuetzle@kip.uni-heidelberg.de

† URL: [www.kip.uni-heidelberg.de/matterwaveoptics](http://www.kip.uni-heidelberg.de/matterwaveoptics)

- [1] See for example D. Preble, *Artforms* (Harper & Row, New York, 1978).
- [2] E. Schrödinger, *Naturwissenschaften* **14**, 664 (1926).
- [3] M.V. Berry and N.L. Balazs, *Am. J. Phys.* **47**, 264 (1979).
- [4] I. Bialynicki-Birula, M. Kalinski and J.H. Eberly, *Phys. Rev. Lett.* **73**, 1777 (1994).
- [5] W.P. Schleich, *Quantum Optics in Phase Space*, (Wiley, Weinheim, 2001).
- [6] M.A. Efremov et al., *Laser Phys.* **13**, 995 (2003); M.V. Fedorov et al., *JETP* **97**, 522 (2003).
- [7] See for example the review by A. Buchleitner, D. Delande and J. Zakrzewski, *Phys. Rep.* **386**, 409 (2002).
- [8] M. V. Fedorov and S. M. Fedorov, *Opt. Exp.* **3**, 27 (1998)
- [9] M. Kalinski et al., *Phys. Rev. A* **67**, 032503 (2003).
- [10] H. Maeda and T.F. Gallagher, *Phys. Rev. Lett.* **92**, 133004 (2004).
- [11] L.G. Hanson and P. Lambropoulos, *Phys. Rev. Lett.* **74**, 5009 (1995).
- [12] A.P. Kazantsev, G.I. Surdutovich and V.P. Yakovlev, *Mechanical Action of Light on Atoms*, (Singapore: World Sci., 1990).
- [13] V.I. Balykin and V.S. Letokhov, *Atom Optics with Laser Light*, (Harwood Academic, Chur, Switzerland, 1995).
- [14] D.O. Chudesnikov and V.P. Yakovlev, *Laser Phys.* **1**, 110 (1991).
- [15] M.V. Berry and D.H.J. O'Dell, *J. Phys A: Math. Gen.* **31**, 2093 (1998).
- [16] M.K. Oberthaler et al., *Phys. Rev. Lett.* **77**, 4980 (1996).
- [17] K.S. Johnson et al., *Science* **280**, 1583 (1998).
- [18] Throughout the paper we use  $\hbar \equiv 1$ .
- [19] A. Scholz et al., *Opt. Comm.* **111**, 155 (1994).
- [20] This conclusion is only valid since our interferometric experiment discussed below exclude additional dynamics of the relative phases between diffraction orders